Characterization of the potential minimum of the Fprime0u+(1D2) ion-pair state of Cl2 using (1+2prime) optical-optical double resonance excitation and mass-resolved ion detection

AIP | The Journal of Chemical Physics

Characterization of the potential minimum of the F′0u+(1D2) ion-pair state of Cl2 using (1 + 2′) optical-optical double resonance excitation and mass-resolved ion detection

Trevor Ridley, Robert J. Donovan, and Kenneth P. Lawley

Citation: J. Chem. Phys. **135**, 104302 (2011); doi: 10.1063/1.3625956
View online: http://dx.doi.org/10.1063/1.3625956
View Table of Contents: http://jcp.aip.org/resource/1/JCPSA6/v135/i10
Published by the American Institute of Physics.

Characterization of the potential minimum of the $F'0_u^+(^1D_2)$ ion-pair state of Cl_2 using (1 + 2′) optical-optical double resonance excitation and mass-resolved ion detection

Trevor Ridley,[a] Robert J. Donovan, and Kenneth P. Lawley
EaStCHEM School of Chemistry, Joseph Black Building, The King's Buildings, Edinburgh EH9 3JJ, United Kingdom

(Received 1 July 2011; accepted 27 July 2011; published online 8 September 2011)

Vibrational levels of the $F'0_u^+(^1D_2)$, $F0_u^+(^3P_0)$, and $D0_u^+(^3P_2)$ ion-pair states of $^{35}Cl_2$ and $^{35}Cl^{37}Cl$ in the range 62 500–67 600 cm^{-1} have been observed using (1 + 2′) optical-optical double resonance excitation with mass-resolved ion detection. The strong $F'0_u^+(^1D_2)/F0_u^+(^3P_0)$ coupling has been modelled by a coupled two-state calculation. An optimized fit of the experimental data used an $F'0_u^+(^1D_2)$ state potential with a T_e of 65 177 cm^{-1} and an R_e of ≈2.636 Å with a coupling constant of ≈430 cm^{-1}. The calculation assigns the first observed members of the $F'0_u^+(^1D_2)$ state progression of $^{35}Cl_2$ and $^{35}Cl^{37}Cl$ at 64 998 and 65 094 cm^{-1}, respectively, as transitions to $v = 0$.
 [doi:10.1063/1.3625956]

I. INTRODUCTION

The $F'0_u^+(^1D_2)$ ion-pair state of Cl_2, formerly labelled $1\,^1\Sigma_u^+$, has been the subject of numerous spectroscopic studies as it is the lowest energy state that is populated by the absorption of a single vacuum ultraviolet (VUV) photon from the ground state. However, since the ion-pair state has a much larger internuclear separation than the ground state, only high-v levels are accessed because transitions to levels near to the potential minimum cannot be observed due to prohibitively small Franck-Condon (FC) factors.

Douglas[1] carried out the first extensive absorption study over the range 69 000–75 000 cm^{-1} and observed that the levels above 73 500 cm^{-1} are strongly coupled to a $4p;0_u^+$ Rydberg state. The potential of the coupled state has been calculated by Wörmer *et al.*[2] from a simulation of the dispersed emission back to the ground state. They assigned the vibrational levels observed in the absorption spectrum as $v = 18$–47. Subsequently, Tsuchizawa *et al.*[3] recorded VUV laser excited fluorescence excitation and (1 + 1′) resonance enhanced ionization spectra of a jet-cooled sample in the same energy region. They compared the position of the observed vibrational levels with those supported by the calculated potential and concluded that the observed-calculated (Obs.-Calc.) values change from +40 to −40 cm^{-1} in the range $v = 30$–38. This, they suggested, meant that there was room for a minor revision of the Wörmer potential.

The calculated potential of the $F'0_u^+(^1D_2)$ state has a minimum around 64 000 cm^{-1} where it is predicted to cross the inner walls of the $D0_u^+(^3P_2)$ and $F0_u^+(^3P_0)$ states, formerly labelled[4] α and γ, respectively, as shown in Fig. 1. This energy region has been studied by one-color, (1 + 2) optical-optical double resonance (OODR) excitation via the unbound portion of the $B0_u^+$ state.[7] Long vibrational progressions up to 72 000 cm^{-1} in both the $D0_u^+(^3P_2)$ and $F0_u^+(^3P_0)$ states are observed directly. In addition, several vibrational levels in the range $v = 6$–16 of the $F'0_u^+(^1D_2)$ state are seen indirectly as a consequence of them being coupled to the $F0_u^+(^3P_0)$ state. While the lowest level of the $F'0_u^+(^1D_2)$ state observed,[7] is ∼2000 cm^{-1} above the predicted origin, significantly perturbed levels in the $F0_u^+(^3P_0)$ state progression do indeed begin around 64 000 cm^{-1}. A further room temperature study of the same energy region has been reported by Ishiwata *et al.*[8] using (1 + 2′) OODR excitation via bound levels of the $B0_u^+$ state with fluorescence detection. They reported that $F'0_u^+(^1D_2)$ state levels were seen directly but these were not published, citing a future publication that we have been unable to find. However, they did conclude that the potential minimum of the $F'0_u^+(^1D_2)$ state might be ∼65 300 cm^{-1}, i.e., ∼650 cm^{-1} higher than proposed by Wörmer *et al.*[2]

In the present paper, we report the observation of vibrational levels of the $F'0_u^+(^1D_2)$ state of jet-cooled Cl_2, both $^{35}Cl_2$ and $^{35}Cl^{37}Cl$, populated by (1 + 2′) OODR excitation via bound levels of the $B0_u^+$ state using mass-resolved ion detection. After an initial analysis in which the lowest energy band observed in the spectra of both isotopomers is assigned to $v = 0$, we present a coupled two-state calculation that models the interaction between the $F'0_u^+(^1D_2)$ and $F0_u^+(^3P_0)$ states. The calculation confirms this vibrational numbering and determines the strength of the coupling.

II. EXPERIMENTAL

The ion-pair state levels are excited by a (1 + 2′) OODR excitation path via bound levels of the $B0_u^+$ state, as illustrated in Fig. 1, and detected by ionization following absorption of two additional photons. A XeCl excimer laser (Lambda Physik EMG 201MSC) simultaneously pumped two Lambda Physik dye lasers; an FL 2002 operating with the dye C102 and an FL 3002E operating with the dyes C102, C2, and C120 provided the pump and probe photons, respectively.

[a]Author to whom correspondence should be addressed. Electronic mail: T.Ridley@ed.ac.uk. Fax: +44-131-6506453.

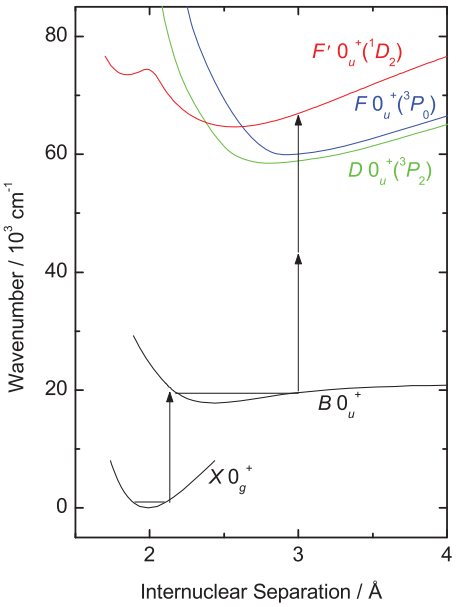

FIG. 1. The molecular potentials of the Cl_2 states discussed in the present study and the $(1 + 2')$ OODR excitation path. The molecular potentials are constructed from the data of Coxon (Ref. 5) ($X0_g^+$ and $B0_u^+$), Al-Kahali (Ref. 6) ($D0_u^+(^3P_2)$ and $F0_u^+(^3P_0)$), and Wörmer *et al.* (Ref. 2) ($F'0_u^+(^1D_2)$). We note that there is a misprint in the published Δr constant in Eqs. (A4) and (A5) of Ref. 2 which should be 5.8×10^{-4} Å.

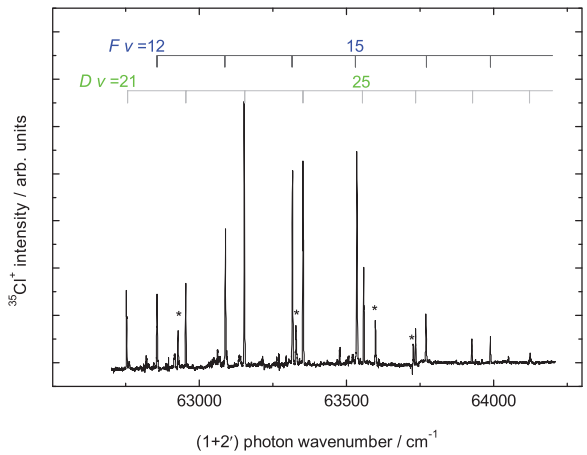

FIG. 2. The 62 700–64 500 cm^{-1} region of the $(1 + 2')$ OODR spectrum of $^{35}Cl_2$ excited via the $B0_u^+ \leftarrow X0_g^+$ (28,0) band. $(1 + (1 + 1'))$ excitations are indicated by asterisks.

The counter-propagating, focussed beams were overlapped in a molecular beam of Cl_2 that was generated by pulsing ~500 Torr of 10% natural Cl_2 in Ar through a General Valve Iota One nozzle into the ionization region of a time-of-flight mass spectrometer (TOFMS). The ion signal from the TOFMS was processed by a Stanford Research SR 250 boxcar integrator and stored on a PC.

$^{35}Cl_2$ and $^{35}Cl^{37}Cl$ isotopomers were studied by collecting $^{35}Cl^+$ and $^{37}Cl^+$, respectively. Although it was usually possible to uniquely excite one of these at the intermediate stage, occasionally the second isotopomer was also weakly excited. To circumvent this problem, all spectra were recorded by simultaneously collecting $^{35}Cl^+$ and $^{37}Cl^+$, and the bands due to the unwanted isotopomer removed by subtracting one spectrum from the other. The laser wavelengths were calibrated from the optogalvanic signal of a neon-filled hollow cathode lamp.

III. RESULTS AND ANALYSIS

A. Assignment of vibrational progressions

The spectra were recorded by exciting the head of an $B0_u^+ \leftarrow X0_g^+$ band and hence typically $J = 0$–4 are excited in the ion-pair state. The term values of the vibrational levels in the ion-pair states are determined by adding the calibrated probe transition wave number, accurate to ± 1 cm^{-1} at the two-photon level, to the term value of the rotationless intermediate state.[5]

Since ionization is a two-photon step, its efficiency can be enhanced by accidental resonances with, most probably, *gerade* Rydberg states resulting in very large variations in the observed ion signal intensities. This phenomenon also means that, in general, very little reliable information can be derived from the relative intensities of the ion signals.

The 62 700–64 500 cm^{-1} region of the $(1 + 2')$ OODR spectrum of $^{35}Cl_2$ excited via the $B0_u^+ \leftarrow X0_g^+$ (28,0) band is shown in Fig. 2. The spectrum contains $D0_u^+(^3P_2)$ and $F0_u^+(^3P_0)$ state progressions with $v = 21$–28 and 12–17, respectively. All of these were seen previously in the $(1 + 2)$ OODR spectrum excited via the continuum of the intermediate state.[7] Several additional weak bands (indicated by asterisks) are observed which are due to $(1 + (1 + 1'))$ excitations, via the same intermediate level, to the same progressions.

The $D(v = 25)$ and $F(v = 15)$ levels are shifted by ~10 cm^{-1} (see Table I) as a result of weak coupling between the $D0_u^+(^3P_2)$ and $F0_u^+(^3P_0)$ states as reported previously.[7] Perturbations of ≤ 10 cm^{-1} between the vibrational levels of these two states are observed throughout the spectra. In all spectra the ladders indicate the observed band positions.

The 64 100–65 800 cm^{-1} region of the $(1 + 2')$ OODR spectrum of $^{35}Cl_2$ excited via the $B0_u^+ \leftarrow X0_g^+$ (20,0) band is shown in Fig. 3(a). As above, the bands indicated by asterisks are due to $(1 + (1 + 1'))$ excitations. As reported previously,[7] the $D0_u^+(^3P_2)$ state progression can easily be identified throughout this region with no larger perturbations than observed to lower energy. The $F0_u^+(^3P_0)$ state progression can also be identified but with perturbations of up to 65 cm^{-1}.

After these assignments, two weak bands at 64 998 and 65 313 cm^{-1} and a medium strong band at 65 576 cm^{-1} remain and consequently we assign them to $(1 + 2')$ excitations of the $F'0_u^+(^1D_2)$ state. In the earlier $(1 + 2)$ study,[7] these $F'0_u^+(^1D_2)$ state levels and the most strongly coupled $F0_u^+(^3P_0)$ state level, $(v = 22)$, were not observed.

The same $(1 + 2')$ photon energy region has been covered using $B(v = 28$ and 15) as the intermediate level. Ion-pair state vibrational levels that are accessed by $(1 + 2')$ excitations appear at the same transition energies in all three spectra, albeit with varying intensities that are dependent on FC factors. As there are no extra bands below 64 998 cm^{-1} in any of these spectra, this band was initially assigned as $F'(v = 0)$.

TABLE I. Transition energies, T_v, of vibrational levels of the $F0_u^+(^3P_0)$ state of $^{35}Cl_2$ and $^{35}Cl^{37}Cl$ observed in the present study and their offsets from those calculated from a cubic polynomial fit of $v = 0$–34.

	$^{35}Cl_2$		$^{35}Cl^{37}Cl$	
v	T_v (cm^{-1})	Obs.-Calc. (cm^{-1})	T_v (cm^{-1})	Obs.-Calc. (cm^{-1})
12	62 855	7	62 816	4
13	63 087	5	63 046	2
14	63 315	1	63 269	− 3
15	63 530	− 12	63 504	6
16	63 771	3	63 721	− 1
17	63 990	− 1	63 939	− 3
18	64 209	− 3	64 158	− 3
19	64 423	− 7	64 367	− 9
20	64 629	− 17	64 573	− 17
21	64 827	− 32	64 773	− 28
22	65 134	64	64 953	− 56
23	65 268	− 10	65 244	28
24	65 485	1	65 432	12
25	65 685	− 4	65 633	11
26	65 920	29	65 863	41
27	66 106	16	66 009	− 11
28	66 274	− 14	66 209	− 7
29	66 462	− 22	66 417	7
30	66 693	15	...	...
31	66 883	12	66 808	16
32	67 065	4	66 980	− 1
33	67 226	− 24	67 154	− 14
34	67 423	− 14	67 350	− 3

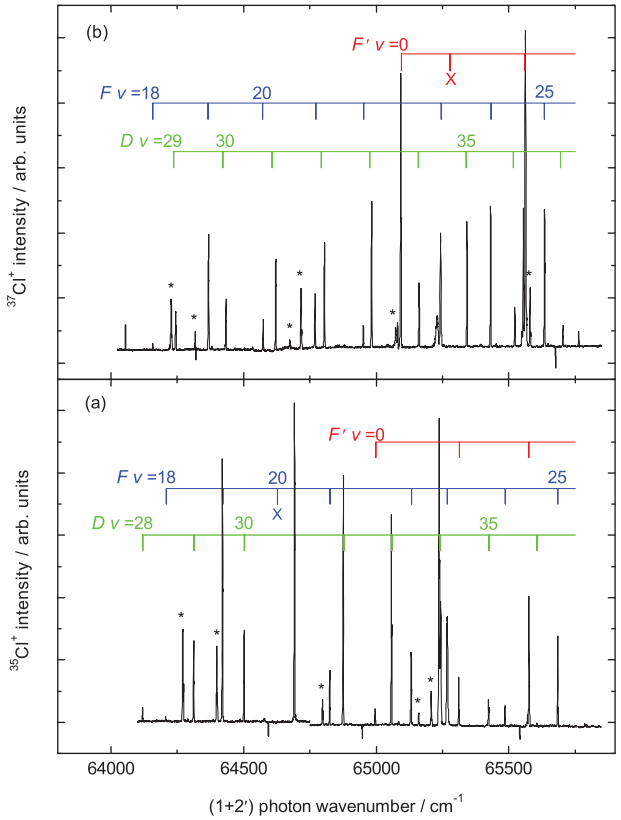

FIG. 3. The 64 100–65 800 cm^{-1} region of the $(1 + 2')$ OODR spectrum of $^{35}Cl_2$ (a) and $^{35}Cl^{37}Cl$ (b) excited via the $B0_u^+ \leftarrow X0_g^+$ (20,0) band. $(1 + (1 + 1'))$ excitations are indicated by asterisks. Crosses indicate the calculated positions of unobserved bands.

The 64 100–65 800 cm^{-1} region of the $(1 + 2')$ OODR spectrum of $^{35}Cl^{37}Cl$ excited via the $B0_u^+ \leftarrow X0_g^+$ (20,0) band is shown in Fig. 3(b). Here, the strong band at 65 094 cm^{-1} is assigned as $F'(v = 0)$. The assignments of the two $v = 0$ bands are confirmed in Sec. III C.

In both isotopomers all three progressions can be followed up to 68 000 cm^{-1}; part of the $^{35}Cl_2$ spectrum is shown in Fig. 4. The transition energies, T_v, of the observed $F0_u^+(^3P_0)$ state vibrational levels of both isotopomers, and those of the $F'0_u^+(^1D_2)$ state are presented in Tables I and II, respectively. Transition energies for some of the higher $F'0_u^+(^1D_2)$ state levels are also shown in Table II in order to show the overlap with the one-photon absorption data.[1,3] The two highest levels shown, $v = 29$ and 30, were previously assigned as $v = 30$ and 31 by Wörmer *et al.*[2]

B. Polynomial fits of the data

We first produced simple polynomial fits of the data in order to determine the magnitude of the perturbations to individual vibrational levels. The term values G_v for $^{35}Cl_2$ and $^{35}Cl^{37}Cl$, relative to the potential minimum of the ground state, were combined in a Dunham expansion of the form

$$G_v(v') = \sum_n Y_{n0}\left[\rho_i\left(v' + \frac{1}{2}\right)\right]^n, \qquad (1)$$

where Y_{n0} is a Dunham parameter and $\rho_i = [\mu(^{35}Cl_2)/\mu_i]^{1/2}$, where μ_i is the reduced mass of a particular isotopomer of Cl_2.

For the $F0_u^+(^3P_0)$ state, the values for $v \geq 18$ were taken from the present work while those for $v = 0$–7 and 12–17 were taken from previous studies.[4,7] All observed values were included in the fit and a cubic polynomial was used to expose the perturbations, in contrast to our previous study where the most perturbed levels were omitted and a six-term polynomial

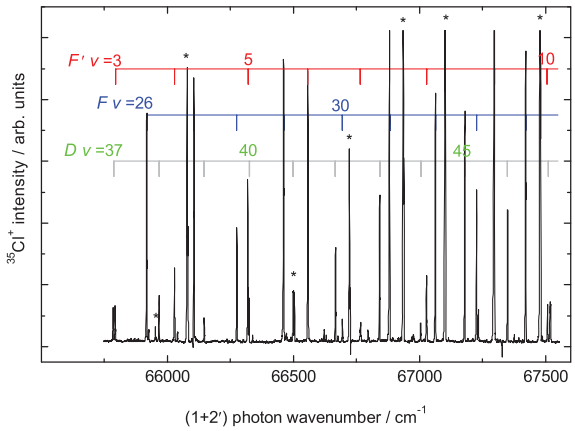

FIG. 4. The 65 500–67 550 cm^{-1} region of the $(1 + 2')$ OODR spectrum of $^{35}Cl_2$ excited via the $B0_u^+ \leftarrow X0_g^+$ (20,0) band. $(1 + (1+1'))$ excitations are indicated by asterisks.

TABLE II. Transition energies, T_v, of vibrational levels of the $F'0_u^+(^1D_2)$ state of $^{35}Cl_2$ and $^{35}Cl^{37}Cl$ observed in the present study and their offsets from those calculated from a quadratic polynomial fit of $v = 0$–10.

	$^{35}Cl_2$		$^{35}Cl^{37}Cl$	
v	T_v (cm^{-1})	Obs.-Calc. (cm^{-1})	T_v (cm^{-1})	Obs.-Calc. (cm^{-1})
0	64 998	− 55	65 094	38
1	65 313	10	…	…
2	65 576	24	65 561	14
3	65 795	− 5	65 762	− 30
4	66 030	− 17	66 040	4
5	66 320	26	66 293	14
6	66 558	18	66 517	− 5
7	66 764	− 21	66 725	− 39
8	67 029	0	…	…
9	67 297	24	67 255	9
10	67 507	− 9	…	…
11	67 725			
12	…			
13	68 234[a]			
14	68 436[a]			
15	68 655[a]			
16	…			
17	69 132[b]			
18	69 386[a]			
19	…			
20	69 799[b]			
…	…			
29	71 750[b,c]			
30	71 942[b,c]			

[a]Reference 7.
[b]Reference 1.
[c]Reference 3.

was used to obtain Dunham coefficients.[7] The differences between the observed values for $v \geq 18$ and those calculated from the cubic fit are shown in Table I. The procedure was repeated for $v = 0$–10 of the $F'0_u^+(^1D_2)$ state using the term values and vibrational numbering determined in the present work where only a quadratic polynomial fit was required and the results are shown in Table II.

C. The coupled two-state calculation

1. Overview

The primary aim is to establish the numbering of the vibrational progression of the $F'0_u^+(^1D_2)$ state where one or two vibrational levels might lie below the apparent origins at 64 998 and 65 094 cm^{-1} in $^{35}Cl_2$ and $^{35}Cl^{37}Cl$, respectively. These could be inaccessible either because of poor FC overlap with the intermediate $B0_u^+$ state vibrational levels used, or because, unlike higher more mixed vibrational levels, they have become nearly pure singlet states and the $B0_u^+$ state is predominantly triplet. The $F0_u^+(^3P_0)$ and $F'0_u^+(^1D_2)$ states are clearly very perturbed as we illustrate above from the offsets of the observed bands from the simple cubic and quadratic fits of the $F0_u^+(^3P_0)$ and $F'0_u^+(^1D_2)$ state vibrational progressions, respectively. The fits show areas of deviation of up to 65 cm^{-1} throughout the region above the crossing of the two states.

Although in principle the $F'0_u^+(^1D_2)$, $F0_u^+(^3P_0)$, and $D0_u^+(^3P_2)$ states all interact in the energy region covered in this paper, the $D0_u^+(^3P_2)$ state is relatively little perturbed and we will attempt to fit the heavily perturbed $F0_u^+(^3P_0)$ and $F'0_u^+(^1D_2)$ progressions by using a vibronic coupling model involving these two electronic states, attributing any residual discrepancies in the fitting to triple interactions with the $D0_u^+(^3P_2)$ state. It is clear that the perturbations do not just involve isolated pairs of vibronic levels in the two electronic states that periodically come into near resonance roughly every 1000 cm^{-1} on the vibrational ladder but that each region of perturbation extends over several vibrational levels (average spacing ~250 cm^{-1}), so that these coupled regions run into each other. We thus need a global rather than a local fit to the data by a procedure that is rapid because the data set contains 28 levels and more than one parameter must be optimized.

2. The global fitting procedure

The wave function of the vth rovibronic level of two interacting $\Omega = 0$ electronic states is

$$\Psi_{vj}(\mathbf{R}, \mathbf{r}) = \left[\psi_{vj}^{(1)}(R)\chi^{(1)}(R, \mathbf{r}) + \psi_{vj}^{(2)}(R)\chi^{(2)}(R, \mathbf{r})\right] \times Y_{jm}(\theta, \phi), \quad (2)$$

where (1) ≡ F, and (2) ≡ F', R is the internuclear separation and $\mathbf{r}$ is a collective electronic coordinate. The electronic wave functions $\chi(R,r)$ are assumed to be normalized at all R and Ψ itself is normalized by requiring $\int_0^\infty \psi_n^{(1)^2} dR + \int_0^\infty \psi_n^{(2)^2} dR = 1$. In a diabatic basis, the electronic wave functions are taken to be independent of the interatomic coordinates $\mathbf{R}$, at least in the coupling region[2,9] and the coupling is attributed to a term $\mathcal{H}^c(R,r)$ in the Hamiltonian. This is appropriate for the present problem because the $F0_u^+(^3P_0)$ and $F'0_u^+(^1D_2)$ states are nominally triplet and singlet, respectively, and the coupling term is then principally the spin-orbit operator, $\mathcal{H}_{s.o}$, leading to a very rapid change in $\chi^{(1)}$ and $\chi^{(2)}$ around the avoided crossing if an adiabatic basis is used. Projecting the wave function for the coupled wave functions (2), $\{\mathcal{H}^v(R) + \mathcal{H}^e(R,r) + \mathcal{H}^c(R,r)\}\mathbf{\Psi}_n = E_n\mathbf{\Psi}_n$ onto the two orthogonal electronic states that are eigenfunctions of $\mathcal{H}^e$ gives, for homogeneous coupling, the standard coupled wave equations for the vibrational eigenfunctions. Putting these in a column vector $\psi = \{\psi^{(1)}, \psi^{(2)}\}$, (see Appendix)

$$\left\{\mathbf{I}\frac{d^2}{d\widetilde{R}^2} + \left[\mathbf{I}\widetilde{E} - \mathbf{V}(\widetilde{R}) - \mathbf{I}\frac{j(j+1)}{\widetilde{R}^2}\right]\right\}\boldsymbol{\psi}(\widetilde{R}) = 0, \quad (3)$$

where the elements of $\widetilde{\mathbf{V}}(R)$ are $\widetilde{V}_{ij}(R) = \langle\chi^{(i)}\widetilde{\mathcal{H}}^e(R,r) + \widetilde{\mathcal{H}}^c\chi^{(j)}\rangle$ with the diagonal elements defining the diabatic potentials and the spin-orbit coupling solely responsible for the off-diagonal elements. In Eq. (3), residual dynamic coupling terms of the type $\langle\chi^{(i)}d\chi^{(j)}/dR\rangle d\psi^{(j)}/dR$ have been omitted. All quantities are dimensionless; $\widetilde{R} = R/s$, $\widetilde{E}$, and $\widetilde{V}_{ij}$ are reduced by $2\mu s^2/\hbar^2$, where s is a length parameter appropriate to the method of solution (see Appendix).

The parameters that can be varied are then the location (T_e, R_e) and shape (ω_e, $\omega_e x_e$) of the upper diabatic potential $V_{11}(R)$ which is assumed to be a Morse function, the position of the inner wall of the lower diabatic state $V_{22}(R)$ relative to the upper diabatic state and the coupling constant, V_{12}, which will be assumed to be independent of R.

3. The $F'0_u^+(^1D_2)$ state origin

The approximate positions of the $F0_u^+(^3P_0)$ and $F'0_u^+(^1D_2)$ potentials, together with their ω_e and $\omega_e x_e$ values are known.[2,7,8] The steeply rising inner wall of the $F0_u^+(^3P_0)$ state crosses the $F'0_u^+(^1D_2)$ state close to its minimum. The $F0_u^+(^3P_0)/F'0_u^+(^1D_2)$ coupling constant, V_{12}, will be of the same order of magnitude as the spin-orbit coupling constant, A, in Cl^+. Applying the Landé interval rule to the (perturbed) term differences $^3P_2 - {}^3P_1$ and $^3P_1 - {}^3P_0$ of the cation gives $A \approx 660$–$690\ cm^{-1}$, and this is taken as an upper limit in our optimization of $V_{12}(R_c)$.

The $F'0_u^+(^1D_2)$ diabatic potential, which is required up to 3000 cm^{-1} above T_e, is approximated by a Morse function with D_e and the exponent α initially determined from the best-fit values $\omega_e = 250\ cm^{-1}$ and $\omega_e x_e = 0.36\ cm^{-1}$ obtained from a quadratic fit of the observed vibrational energy levels. The initial choice of $F0_u^+(^3P_0)$ state diabatic potential was that given by Al-Kahali,[6] but this is essentially an adiabatic potential that was derived from a fit of the smoothed vibrational progression of the $F0_u^+(^3P_0)$ state with strongly perturbed levels omitted. The knot points near the potential minimum are quite tightly determined by the lowest vibrational levels of the $F0_u^+(^3P_0)$ state and the inner wall was smoothly modified to pass through the $F'0_u^+(^1D_2)$ state near its minimum. Solving the two uncoupled vibrational wave equations for energies in the region of $F'(v = 0)$, $F(v = 21, 22)$ indicates that the overlap of the two wave functions $\langle 21|0\rangle$ and $\langle 22|0\rangle$ are both ~0.2, falling to ≤ 0.1 for $F'(v = 10)$. Thus to achieve a displacement of the order of those observed, say 40 cm^{-1}, would require $V_{12}(R_c) \geq 200\ cm^{-1}$ (the lower limit only applying if two states in exact resonance interact and neighbouring vibronic states exact no influence).

T_e for the $F'0_u^+(^1D_2)$ state was first located at 64 630 cm^{-1} to coincide with Wörmer's[2] value and which corresponds to placing $F'(v = 0)$ two quanta below our lowest level. Even with the low value of V_{12} of 200 cm^{-1}, the $F0_u^+(^3P_0)$ state progression was markedly disturbed by ~20 cm^{-1} around $v = 19, 20$, whereas the major perturbation in the $F0_u^+(^3P_0)$ state progression is at $v = 21$–23. Furthermore, $F'(v = 0)$ had ~30% $F0_u^+(^3P_0)$ character and so should have been easily accessible at around 64 490 cm^{-1} in our excitation scheme. Raising $T_e(F')$ by one quantum (~250 cm^{-1}) from Wörmer's value to 64 890 cm^{-1} shows that $F'(v = 0)$ now has ~35% $F0_u^+(^3P_0)$ character and should be visible at around 64 760 cm^{-1}. Finally, with $T_e(F')$ at ~65 150 cm^{-1}, the lowest (displaced) $F'0_u^+(^1D_2)$ level has $T_0 = 65\,003\ cm^{-1}$, in approximately the observed position and ~26% $F0_u^+(^3P_0)$ character, so accessible from the $B0_u^+$ intermediate state. More detailed fitting thus proceeded with the assumption that the lowest observed $F'0_u^+(^1D_2)$ level at 64 998 cm^{-1} is indeed $v = 0$.

4. The optimized fit

In order to optimize the fit under coupled conditions, some guidance as to the range of parameter values is helpful, but uniqueness of fit cannot be guaranteed. If two diabatic vibronic levels $F(v)$ and $F'(v')$ come into near resonance, the maximum displacement is $\pm\langle v|V_{12}(R)|v'\rangle$. If the electronic coupling is assumed to be independent of R so the off-diagonal elements of $V_{12}(R)$ are largely determined by the overlap of the vibrational wave functions in a localized region around the avoided crossing R_c, then

$$\langle v|V_{12}(R)|v'\rangle \approx V_{12}(R_c)\langle v|v'\rangle. \tag{4}$$

From Table I it can be seen that the first major perturbation of the $F0_u^+(^3P_0)$ state progression occurs around $v = 21$ at 64 827 cm^{-1} and the lowest observed level of the $F'0_u^+(^1D_2)$ state, now labelled as $v = 0$, lies at 64 998 cm^{-1} ($G_v = 65\,277\ cm^{-1}$). Thus to make a preliminary estimate of the magnitude of the parameter $V_{12}(R_c)$ from the observed value of ΔE for $F'(v = 0)$ we require the FC factor for the overlap of $F(v = 21)$ and $F'(v = 0)$. Solving the uncoupled wave equations with the trial potentials for the $F0_u^+(^3P_0)$ and $F'0_u^+(^1D_2)$ states outlined above shows that $F'(v = 0)$ probably lies between $v = 21$ and $v = 22$ of the $F0_u^+(^3P_0)$ state. Using the vibrational eigenfunctions of the uncoupled states gives $\langle 21|0\rangle = 0.21$ and $\langle 22|0\rangle = 0.20$, so to achieve a displacement of, say, 50 cm^{-1} in either series will require $V_{12}(R_c) \geq 250\ cm^{-1}$, the lower limit only applying if two states in exact resonance interact.

The optimized potential parameters for the diabatic $F0_u^+(^3P_0)$ and $F'0_u^+(^1D_2)$ states are listed in Table III. The adjustable parameters were small shifts in R_e and T_e of the $F'0_u^+(^1D_2)$ state (R_e of the $F0_u^+(^3P_0)$ state was kept fixed at 2.937 Å, the value reported by Ishiwata *et al.*[4]) and the strength of the coupling term. There is some correlation between the values of T_e, the position of the inner wall of the $F0_u^+(^3P_0)$ state potential and V_{12}, but T_e is located to perhaps $\pm 20\ cm^{-1}$. A range of V_{12} values between 420 and 440 cm^{-1} were found to give acceptable fits. Taking the value of 430 cm^{-1} gave standard deviations, σ, for the combined $F0_u^+(^3P_0)$ and $F'0_u^+(^1D_2)$ vibrational data given in Tables I and II of 3.6 and 5.4 cm^{-1} for the $^{35}Cl_2$ and $^{35}Cl^{37}Cl$ isotopomers, respectively. The value of σ for the cubic polynomial fit of the $F0_u^+(^3P_0)$ state T_v values of the two isotopomers described above is 17 cm^{-1}. The value of σ for the quadratic fit of the equivalent $F'0_u^+(^1D_2)$ state T_v values is 24 cm^{-1}. Furthermore, the maximum deviation from a smooth polynomial fit of the $F0_u^+(^3P_0)$ state is 65 cm^{-1} for $^{35}Cl_2$ and 56 cm^{-1} for $^{35}Cl^{37}Cl$ which is reduced to 8 and 10 cm^{-1}, respectively, in the coupled states fit. The predicted positions of the $F0_u^+(^3P_0)$ and $F'0_u^+(^1D_2)$ state levels that remain poorly fitted are in near coincidence with the positions of $D0_u^+(^3P_2)$ state levels calculated from a polynomial fit. For example, in $^{35}Cl_2$, $F'(v = 8)$ and $D(v = 44)$ are predicted to lie at 67 021

TABLE III. Parameters derived from the optimized fit under coupled conditions.

(i) Morse parameters for the diabatic $F'0_u^+(^1D_2)$ state and the ω_e and B_e values derived from them

D_e (cm^{-1})	α ($Å^{-1}$)	R_e (Å)	T_e (cm^{-1})	ω_e (cm^{-1})	B_e (cm^{-1})
20 500	0.904	2.636	65 177	254	0.1385

(ii) Dunham coefficients for the diabatic $F0_u^+(^3P_0)$ state

Y_{00} (cm^{-1})	Y_{10} (cm^{-1})	Y_{20} (cm^{-1})	Y_{30} (cm^{-1})	Y_{40} (cm^{-1})
59 945.7	278.0891	−1.9216	0.01306	-4.34792×10^{-5}
Y_{01} (cm^{-1})	Y_{11} (cm^{-1})	Y_{21} (cm^{-1})	Y_{31} (cm^{-1})	Y_{41} (cm^{-1})
0.11179	−0.00182	7.41196×10^{-5}	-2.0907×10^{-6}	2.2070×10^{-8}

and 67 014 cm^{-1}, respectively. The observed level of the former is pushed up by 8 cm^{-1}, while that of the latter is pushed down by the same amount. In $^{35}Cl^{37}Cl$, $F(v = 29)$ and $D(v = 41)$ are predicted to lie at 66 407 and 66 403 cm^{-1}, respectively; the observed levels are offset by +10 and −13 cm^{-1}.

As the T_e of the optimized potential of the $F'0_u^+(^1D_2)$ state is ∼550 cm^{-1} higher than that reported by Wörmer *et al.*,[2] i.e., well outside their quoted uncertainty of ±50 cm^{-1}, we should consider the sources of the discrepancy in their calculation which involved the simulation of $F'0_u^+(^1D_2) \rightarrow X0_g^+$ emission. The largest uncertainty appears to be in the use of a Hulbert-Hirschfelder potential to approximate the $X0_g^+$ state potential energy curve, the parameters of which were not allowed to vary.

Fluorescence from $F'(v = 39)$ at wavelengths corresponding to a classical point of transition around R_e of the $F'0_u^+(^1D_2)$ state produces $Cl_2(X)$ very close to dissociation at around 20 000 cm^{-1}. The structure in the dispersed fluorescence is then sensitive to small displacements of the inner wall of the ground state potential which may not be accurately modelled by the Hulbert-Hirschfelder potential in this energy region. Additionally, if there is appreciable coupling of the emitting $F'(v = 39)$ level with the $F0_u^+(^3P_0)$ manifold in which it is embedded, then a further shift is induced in the structure of the $F'0_u^+(^1D_2) \rightarrow X0_g^+$ emission which may have been compensated for by adjusting T_e or R_e of the $F'0_u^+(^1D_2)$ state.

IV. CONCLUSIONS

We have observed vibrational levels of the $F'0_u^+(^1D_2)$, $F0_u^+(^3P_0)$, and $D0_u^+(^3P_2)$ states of $^{35}Cl_2$ and $^{35}Cl^{37}Cl$ in the range 62 500-68 000 cm^{-1} using (1 + 2′) OODR excitation with mass-resolved ion detection. The first members of the $F'0_u^+(^1D_2)$ state progression of $^{35}Cl_2$ and $^{35}Cl^{37}Cl$ are observed at 64 998 and 65 094 cm^{-1}, respectively, which we therefore assign to $v = 0$. The $F'0_u^+(^1D_2)$ and $F0_u^+(^3P_0)$ states are shown to be strongly coupled as reported previously[2,3,7,8] causing displacements of up to ±65 cm^{-1} from polynomial fits of the vibrational energy levels. An optimized fit of the experimental data by a coupled two-state calculation used an $F'0_u^+(^1D_2)$ state diabatic potential with a T_e of 65 177 cm^{-1} and an R_e of ≈2.636 Å with a coupling constant of ≈430 cm^{-1}. This value of T_e is 546 cm^{-1} higher than that deduced from an analysis of dispersed fluorescence from a high vibrational level 8000 cm^{-1} above T_e. The calculation also confirmed that the first observed members of the $F'0_u^+(^1D_2)$ state progressions are the T_0 bands.

APPENDIX: NUMERICAL IMPLEMENTATION

We solve the coupled equation (2) by representing the continuous functions $\psi_{1,n}$ and $\psi_{2,n}$ by a column vector **w** of values on a common grid of N equally spaced radial points, $y_1 = \psi^{(1)}(R_1)$, $y_2 = \psi^{(2)}(R_1)$, $y_3 = \psi^{(1)}(R_1 + s)$, …, $y_{2N} = \psi^{(2)}(R_1 + Ns)$. The second derivative is replaced by the second order central difference at each grid position, $d^2\psi^i/dr^2|_{R_n} = (\psi_{n-1}^{(i)} - 2\psi_n^{(i)} + \psi_{n+1}^{(i)})/s^2$. The eigenvalue problem then reduces to the algebraic problem of finding the roots of a pentadiagonal matrix.[10]

The diagonal elements contain $w_n^{(i)} = V_{ii}(R_n) + j(j+1)/R_n^2$ defining the two diabatic potentials and the coupling is provided by $x_n = V_{ij}(R_n)$ alternating with zeros in the first off-diagonal positions $(n,n\pm1)$. The coupled two-state wave equation (3) then becomes

$$\begin{pmatrix} w_1^{(1)}+2-E & x_1 & -1 & 0 & \cdots & \cdots & \cdots \\ x_1 & w_1^{(2)}+2-E & 0 & -1 & 0 & \cdots & \cdots \\ -1 & 0 & w_2^{(1)}+2-E & x_2 & -1 & 0 & \cdots \\ 0 & -1 & x_2 & w_1^{(2)}+2-E & 0 & -1 & \cdots \\ \cdots & \cdots & \cdots & \cdots & \cdots & \cdots & \cdots \\ \cdots & \cdots & \cdots & 0 & -1 & x_N & w_N^{(2)}+2-E \end{pmatrix} \begin{pmatrix} y_1 \\ y_2 \\ y_3 \\ y_4 \\ \cdots \\ y_{2N} \end{pmatrix} = 0.$$

The roots E_n in a selected energy range are quickly found by bisection to any required precision, δE, that is consistent with step length, s. Typically, $s = 10^{-3}$ Å and $\delta E = 10^{-1}$ cm^{-1} were used. Eigenfunctions, which are only required in squared form for the weights of the two electronic states in a given vibronic level,

$$P_{vj}^{(1)} = \frac{\sum_{n=odd}^{2N-1} y_n^2}{\sum_{n=odd}^{2N-1} y_n^2 + \sum_{n=even}^{2N} y_n^2}$$

are found subsequently for selected eigenvalues as the product of the forward and back determinants at each tabulated position.

[1]A. E. Douglas, Can. J. Phys. **59**, 835 (1981).
[2]J. Wörmer, T. Möller, J. Stapelfeldt, G. Zimmerer, D. Haaks, S. Kampf, J. Le Calvé, and M. C. Castex, Z. Phys. D, At. Mol. Clusters **7**, 383 (1988).
[3]T. Tsuchizawa, K. Yamanouchi, and S. Tsuchiya, J. Chem. Phys. **93**, 111 (1990).
[4]T. Ishiwata, I. Fujiwara, T. Shinzawa, and I. Tanaka, J. Chem. Phys. **79**, 4779 (1983).
[5]J. A. Coxon, J. Mol. Spectrosc. **82**, 264 (1980).
[6]M. S. N. Al-Kahali, Ph.D. thesis, University of Edinburgh, 1996.
[7]M. S. N. Al-Kahali, R. J. Donovan, K. P. Lawley, T. Ridley, and A. J. Yarwood, J. Phys. Chem. **99**, 3978 (1995).
[8]T. Ishiwata, T. Shinzawa, J. Si, K. Obi, and I. Tanaka, J. Mol. Spectrosc. **166**, 321 (1994).
[9]D. Stahel, M. Leoni, and K. Dressler, J. Chem. Phys. **79**, 2541 (1983).
[10]K. P. Lawley, J. Comput. Phys. **70**, 218 (1987).